The Helmet Fit Index
A Method for the Computational Analysis of Fit between Human Head Shapes and Bicycle Helmets

Thierry Perret-Ellena, Aleksandar Subic, Toh Yen Pang and Helmy Mustafa
RMIT University, School of Aerospace, Mechanical And Manufacturing Engineering, Building 251, Level 3 Bundoora Campus East, Plenty Road Bundoora Vic 3083, Melbourne, Australia

Keywords: 3D Anthropometry, Reverse Engineering, Gap Analysis, Bicycle Helmet Fit, 3D Scanner.

Abstract: While a bicycle helmet protects the wearer's head in the event of a crash, not every user benefits to the same extent when wearing the headgear. A proper fit with the cyclist's head is found to be one of the most important attributes to improve protection during impact. A correct fit is defined as a small and uniform distance between the helmet liner and the wearer's head shape, with a broad coverage of the head area. The scientific community has recognised the need for improved fitting, but in-depth methods to analyse and compare the fit performance of distinct helmets models are still absent from the literature. We present a method based on 3D anthropometry, reverse engineering techniques and computational analysis to redress this shortcoming. As a result of this study, we introduce the Helmet Fit Index (HFI) as a tool for fit analysis between a helmet model and a human head. It is envisaged that the HFI can provide detailed understanding of helmet efficiency regarding fit and should be used during helmet development phases and testing.

1 INTRODUCTION

Bicycle helmets play an important role in cyclist safety during crashes (Attewell et al., 2001); (Abu-Zidan et al., 2007); (Cripton et al., 2014), where they reduce the risk of head and facial injury significantly across the whole cyclist population (Thompson et al., 1999). However, studies showed that a poor helmet fit on the wearer's head may decrease its safety benefits during a crash event (Romanow et al., 2014) (Rivara et al., 1999).

Poor helmet fit may be attributed in two ways. First, the helmet could be worn incorrectly, titled either forward or backward, with the chin strap unfastened or, with the helmet worn back to front. An observational study from Canada reported that 15% of bike users worn their helmet incorrectly (Hagel et al., 2010). Wearing under or over-sized helmets is also considered as inappropriate usage. Second, helmet sizes and shapes available to the public might not be suitable for the full diversity of head morphologies. Indeed, for some users there is either a large gap between the inner liner and the head, or a low coverage of the skull area with significant unprotected regions on the head. Rivara et al. (1999) found that during crash events, children with head injuries had large open gaps between their head and the helmet, compared to those without head injuries.

While the misuse of bicycle helmets is rectifiable through school-based education programs, government and helmet manufacturer advertising, and store advice and information, the mismatch between head shapes and helmet liners seems to be related to the design of helmets.

Nowadays, protective equipment are designed and tested on standard mannequin heads called headforms (Ball, 2009) (Zhuang et al., 2010), which aim to represent the full range of head dimensions, geometries and shapes within a population. Although two headform standards have been proposed in the past (ISO/R1511:1970 and ISO/DIS 6220:1983), neither of them were adopted as an international standard. However, the draft ISO/DIS 6220:1983 has become a consensus international standard for many countries and served as a reference for the development of their own standard. For instance, Australia developed the AS/NZS 2512.1:2009 *Methods of testing protective helmets Part 1: Definitions and headforms* (Standards Australia, 2009), where five headform sizes are presented, namely A, E, J, M and O. Interestingly,

Perret-Ellena T., Subic A., Yen Pang T. and Mustafa H..
The Helmet Fit Index - A Method for the Computational Analysis of Fit between Human Head Shapes and Bicycle Helmets.
DOI: 10.5220/0005084101450153
In *Proceedings of the 2nd International Congress on Sports Sciences Research and Technology Support* (icSPORTS-2014), pages 145-153
ISBN: 978-989-758-057-4

the ISO draft was itself founded from the first set of test headforms produced by the UK Transport Road Research Laboratory in the 1950s' (British Standards Institution, 2006). One may think that designing bicycle helmets on anthropometric measurements from the 1950s British workforce would not fully encompass the variability on head shapes in today's population. It might lead to improper helmet fit for a large proportion of cyclists.

In order to go beyond the errors in the anthropometric data and to match the majority of people head shapes, designers have been creating helmet liners with significant offset distance from the standard headform surfaces. This designing approach also ensures the highest proportions of users are captured with the smallest numbers of sizes. It is common for helmet manufacturers to only provide one or two sizes for both male and female populations. Thick foam pads are then added to fill the gaps between the liners and wearer's head. While this approach noticeably improves comfort and allows a minimum gap for air circulation, it does not reduce front-to front, side-to-side, or rotational movements that are responsible for poor helmet fitting. It is apparent that such an approach leads to improper helmet fit for a large range of consumers.

Even with a widely recognised poor head-fitted bicycle helmet design (Robinette and Whitestone, 1994), accurate techniques to quantify the adequacy or inadequacy of fit for a distinct person and a distinct helmet are still tedious and inaccurate, and are not in line with today's technology. The distance between the inside of the helmet and the skull of the user is measured using depth probes through holes drilled in the helmet. Only recently 3D scanners have been introduced to accurately compute standoff distances of ballistic helmets (Meunier et al., 2000).

The paper aims to present a method of estimating the 'fit score' of bicycle helmets for unique human head shapes. Based on 3D anthropometric studies, a set of reverse engineering tools and computational techniques was developed to evaluate the fit from the combination of one helmet and one individual's head. We introduced the Helmet Fit Index (HFI) that can be used for statistical analysis of fit on a defined population and the comparison of different headgear models.

2 METHOD

The helmet fit analysis method consisted of four distinct steps: (1) Anthropometry data of participants were recorded and processed using a handheld or rotating 3D scanner and post processing software, (2) bicycle helmets were digitised using a higher-end, fixed 3D scanner, which generated scans with greater accuracy and resolution, (3) both scans were positioned in relation to a third intermediary 3D scan, and (4) multiple computational analyses were performed to compute the HFI for each participant.

2.1 3D Anthropometry: Data Collection and Processing

The Artec Eva™ 3D scanner was used for the anthropometric study. As a handheld white light scanner, it can produce accurate point clouds up to one hundred micrometres at a half a millimetre resolution. It is completely portable and utilises surface geometry and texture algorithms to align itself in space and therefore does not require any targets to be placed on the scanned area.

During the scanning process, participants were asked to sit straight and look at a fixed point on the wall with his/her usual facial expression. The posture position and scanning techniques were in accordance with the requirements of ISO 20685:2010(E*) 3-D scanning methodologies for internationally compatible anthropometric databases* (International Organization for Standardization, 2010b). Participants were asked to wear standard wig caps on their heads and over their ears to avoid hair irregularities on the scanned geometry. The scanner can record single scan at a rate of fifteen frames per second for about thirty seconds and automatically aligned the frames while scanning (Figure 1(a)).

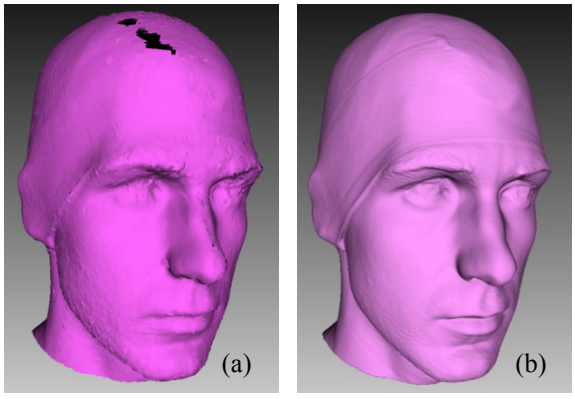

Figure 1: (a) Rough alignment of 532 single scans, (b) Watertight scan.

Fine alignment algorithms and clean-up were then performed on the individual shots before the hundreds of scans were merged together in a smooth

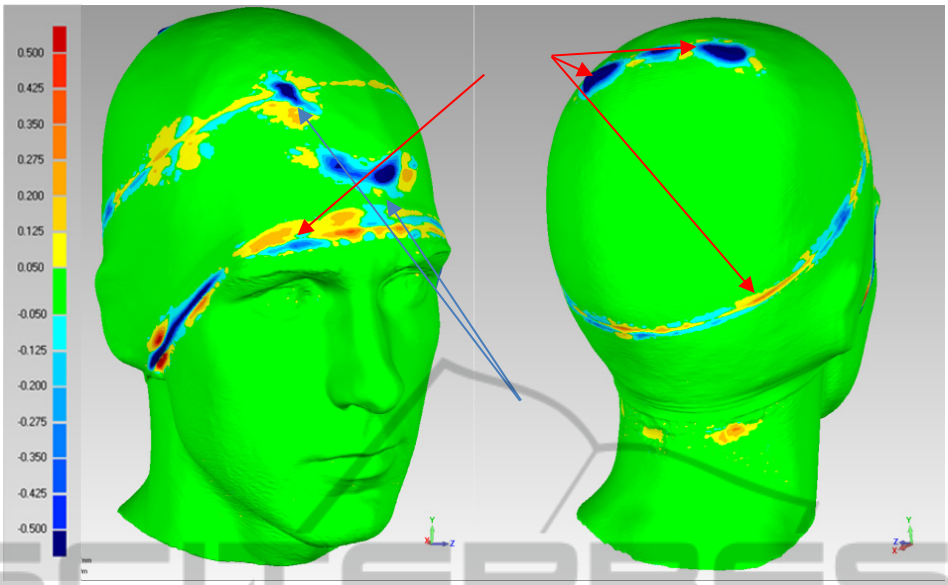

Figure 2: Deviation Analysis. Green is within the allowed distance variation.

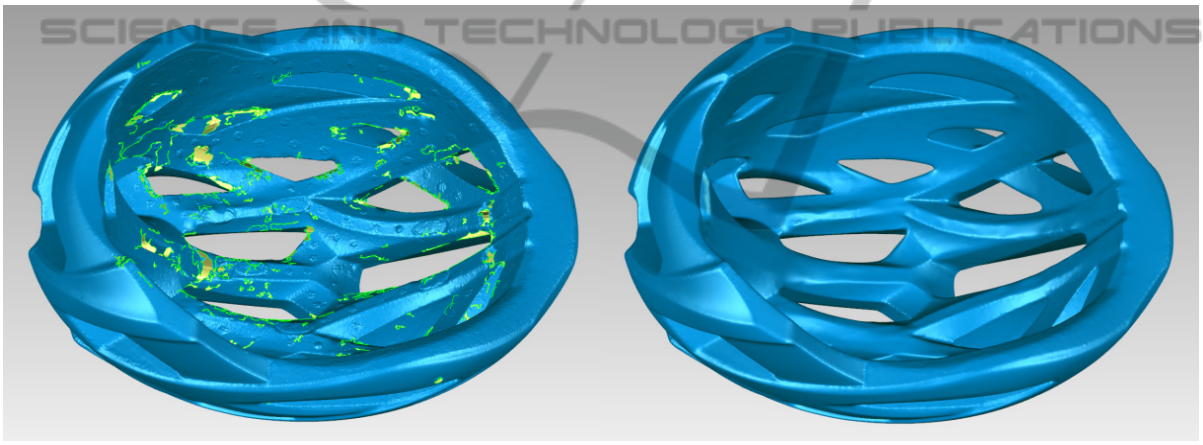

Figure 3: Met Kaos size M. Left: Merged scans with holes, Right: Final helmet mesh (holes filled, repaired, smoothed out, re-wrapped).

fusion procedure. Mesh was generated and missing areas were filled to create a single watertight scan as presented in Figure 1(b).

Mesh was then exported to Geomagic Studio 12® for further processing. Hair bumps and fabric folds were removed while the scan was smoothed out by minimising angles between individual polygons. The deviation analysis tool was used to ensure that the modification to the mesh had not excessively distorted the original scanned head shape. The maximum deviation distance for non-hair bumps or fabric fold areas was set to $\pm 50 \mu m$. Figure 2 shows the deviation analysis computed after the post processing has been completed. The green areas are deviation within the threshold value. Higher deviation values (highlighted in red and blue) arose from folds in the wig cap fabric and uneven surfaces due to hair irregularities.

2.2 Bicycle Helmet Reverse Engineering and Data Preparation

The tested helmet was digitised with an advanced 3D scanner (HDI Advance from LMI Technologies), which has a high level of scan accuracy and quality when dealing with more complex geometries. The average point-to-point resolution is $75 \mu m$ with an accuracy of up to $45 \mu m$. Seventy single scans on average were recorded for each helmet. Foam pads and the adjusting system were removed either (i)

physically before the scan, or (ii) digitally during the post processing procedure. The scan images were merged, repaired and cleaned-up in Geomagic studio 12® (Figure 3 shows a scanned Met Kaos helmet model). The clean-up process involved the following: (a) repaired the mesh to remove spikes and non-manifold triangles, (b) filled holes with curvature continuity constraints with the adjacent geometry, (c) reconstructed the fillets and sharp edges, and (d) re-wrapped the mesh with new vertices for uniform spacing. The final repaired mesh produced approximately two million triangles.

When performing the gap analysis on the inside surfaces of the helmet liner, we duplicated the mesh on the software tree and kept only the regions supposedly in contact with the cyclists' head. Figure 4 illustrates the final inside surface of the same helmet after careful trim and with proper area selection.

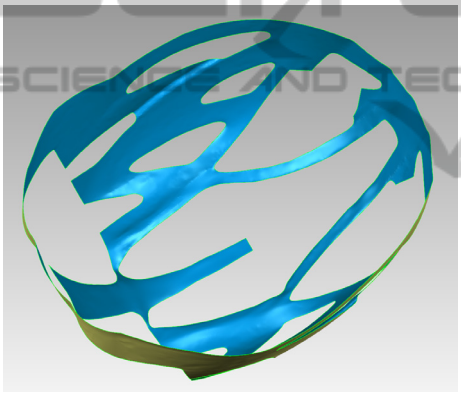

Figure 4: Met Kaos, inside mesh.

The fit analysis was performed both globally and locally as we predicted the fit to be dissimilar throughout the whole head shape. The inside mesh of the helmet liner was therefore further divided into five regions, namely front, top, right, left, and back as shown in figure 5.

2.3 Scans Alignment

In order to analyse the gap between the head and the inside surface of the helmet liner, the fine helmet mesh was assembled in position with the head scan. Instead of manually aligning the two meshes together, we utilised a third–intermediary scan to properly position the helmet with the participant's head. Participants were scanned a second time with the tested helmet model fitted on their heads. During the scan, participants were asked to reproduce the same posture and facial expression as the first scan

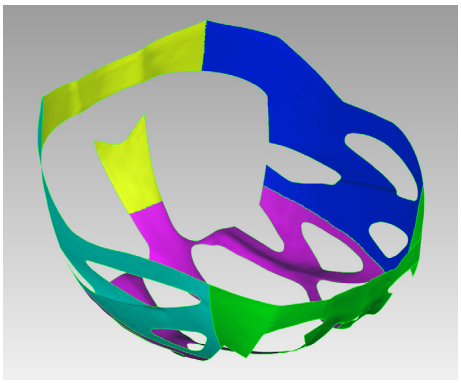

Figure 5: Met Kaos regions. green = front, pink = top, blue = right, turquoise = left, yellow = back.

while a rough scan was performed. Foam pads, chin strap and the adjusting system were excluded during the fitting process as we only aimed to investigate how well the helmet liner matched with the head shape of the participant.

All three scans (Figure 6) were then aligned using the n-points manual registration and the global registration algorithms within Geomagic Studio 12®. The alignment process was split into two stages: (i) aligned the head scan and the intermediary scan (Figure 7) using the face polygons of the participant, and (ii) aligned the helmet scan with the intermediary scan (Figure 8).

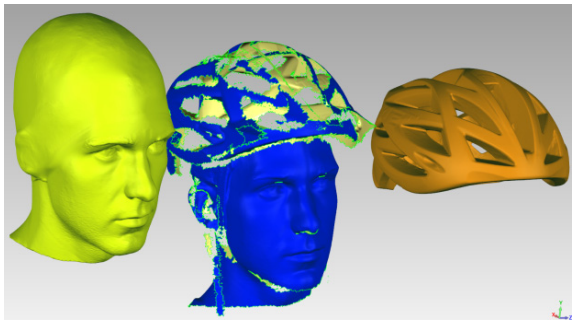

Figure 6: Three scans for alignment. Yellow: head scan. Blue: Intermediary scan. Orange: Helmet scan.

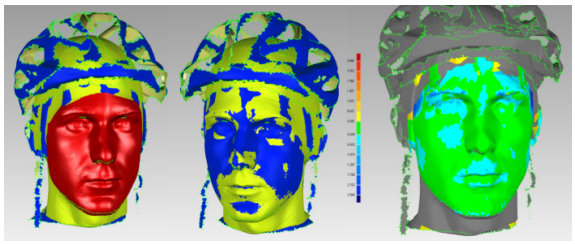

Figure 7: Head/intermediary scan alignment. From left to right: Face polygons selection for global registration (red), good overlapping between the meshes, deviation analysis (green is < to ±0.1mm).

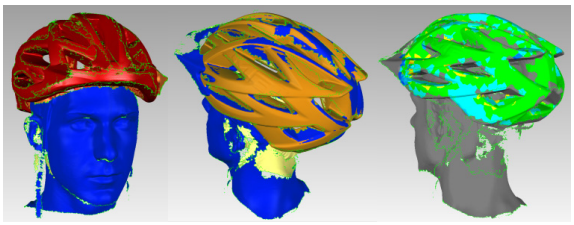

Figure 8: Intermediary/helmet scan alignment. From left to right: Helmet polygons selection for global registration (red), good overlapping between the meshes, deviation analysis (green is < to ±0.2mm).

After the two-stage alignment process, the intermediary scan was removed, and the head and helmet scans were now aligned accurately (Figure 9). This allowed the gap between the head and helmet to be inspected and analysed.

Figure 9: Final alignment.

2.4 Gap Analysis

In this analysis, the gap distribution between the head mesh and the inside of the helmet was calculated. Two parameters were determined: (i) the Standoff Distance (SOD), which was defined as the average minimal distance to the head shape amongst all the points that defined the inside mesh of the liner, and (ii) the Gap Uniformity (GU), which was the standard deviation of the gap distribution, and defined as the dispersion from the average.

Figure 11: Gap analysis on the right region, and the SOD and GU were 6.11mm and 1.84mm, respectively.

A distance analysis tool from CATIA V5R21 (Dassault Système) was used to measure the gap between the trimmed head and the inside liner meshes. We first analysed the gap to look for any negative values that would indicate a crush between the two meshes. Interference might arise either from inaccurate alignment between the meshes, or the hair

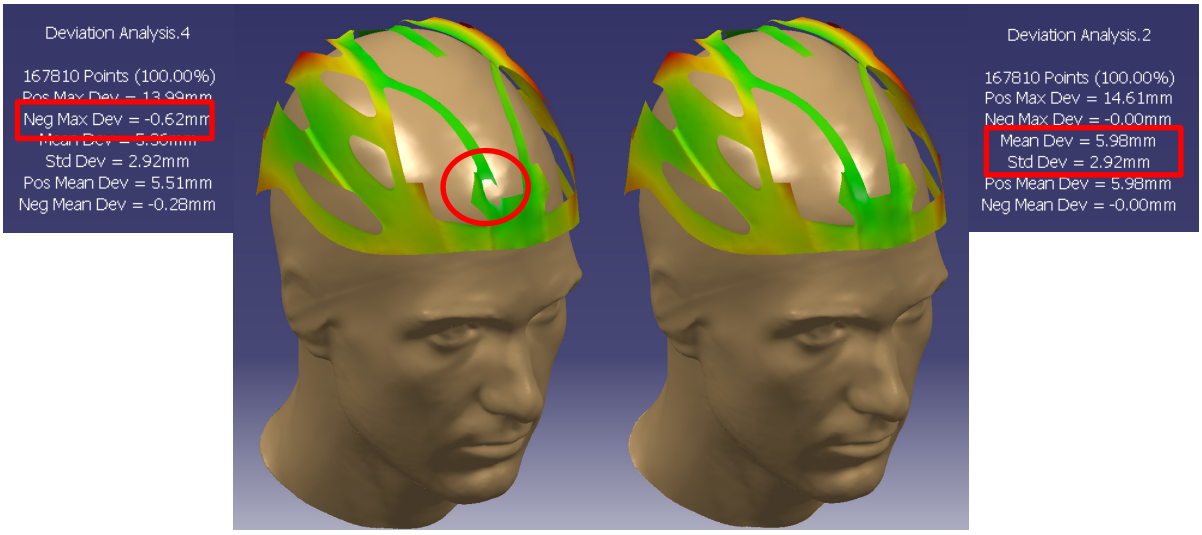

Figure 10: Gap analysis texture maps before (interferences marked in red circle) and after offset. Hair thickness was 0.62mm, and SOD and GU were 5.98mm and 2.92mm, respectively.

thickness of the participant. The participant's hair was likely to be compressed under the helmet's weight during the fitting and this extra thickness of hair was considered during the gap analysis. Outliner points were removed from the result and the head scan was offset by the negative maximum deviation. The hair thickness was assumed to be uniform across the whole head. Distance analysis was then recalculated and the SOD and GU were recorded. Figure 10 shows the gap analysis with colour texture maps before and after the hair thickness was offset.

Furthermore, similar deviation analyses were conducted on the five local regions, and the SOD and GU were recorded. Figure 11 depicts a gap analysis of the right region.

2.5 Proportion of Head under Helmet Protection

Ideally, the helmet should cover as much skull area as possible to provide maximum protection to the wearer. However, for some human head shapes, helmet models might provide only minimal total coverage area and put the wearer at increased risk of injury. The AS/NZS 2512.1:2009 *Methods of testing protective helmets Part 1: Definitions and headforms* (Standards Australia, 2009) defines a test line around the head where the helmet is supposed to extend. The dimensions for the test line were based on the Bitragion coronal and inion arcs, and the mid-sagittal arc. We added the dimensions of the head length, breadth and circumference to define, for each participant, an area that should be under the helmet protection (magenta area in Figure 12(a)).

By projecting the boundary edges of the inside liner into the test area, we could compute the proportion of the head mesh under helmet protection (green area in Figure 12(b)). We named this third fit parameter the Head Protection Proportion (HPP).

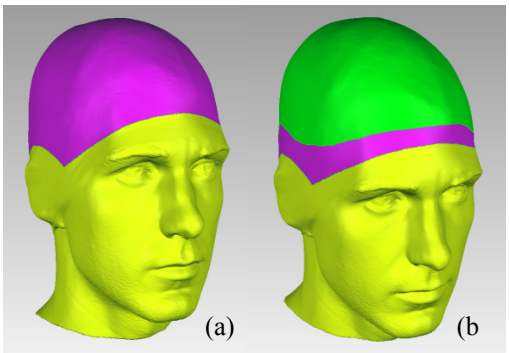

Figure 12: (a) Test area in magenta, (b) Actual helmet protection area in green.

2.6 Helmet Fit Index

The Helmet Fit Index (HFI) aims to provide a fit 'score' for the combination of one specific helmet model and a human head. This index was developed on a scale from 0 (excessively poor fit) to 100 (perfect fit). The probability density function, f, of an exponential distribution was used to generate the index was described as:

$$f(x;\lambda) = \begin{cases} \lambda * \exp(-\lambda x) & x \geq 0, \\ 0 & x < 0. \end{cases} \quad (1)$$

Where $\lambda > 0$ was the parameter of the distribution called the rate parameter.

The probability density function was established on the exponential distribution rather than the log-normal distribution as its right tail is relatively short and may be considered as having moderate skew (i.e. few outliners). A distribution with fewer outliners will produce more statistical significant results.

x was defined as a function of the SOD, GU, and HPP. It tends to approach 0 when the fit is improved.

The SOD optimal value should be greater than zero to allow thermal control throughout the helmet and the addition of thin foam paddings for comfort. However, previous research showed that an excessive standoff distance would decrease the helmet protective function during crashes (Rivara et al., 1999). Therefore, we set the SOD to be optimum when it ranged between 4 and 8mm.

The GU was a key parameter when analysing the dispersion of the distance distribution. Seemingly, the fit is optimised when the standoff distance is uniformly distributed over the whole liner surface, which equivalent to a lower deviation from the mean. Hence, the gap becomes more uniform when the GU gets closer to zero. Likewise, fit improves when the HPP becomes closer to 1, which corresponding to a higher coverage area of the head provided by the helmet.

The fit parameter, x, was defined as:

$$x = \begin{cases} a * (|SOD - 6| - 2) + \dfrac{b * GU}{HPP} \\ \qquad for\ 4 > SOD > 8 \\ \dfrac{b * GU}{HPP} \\ \qquad for\ 4 \leq SOD \leq 8 \end{cases} \quad (2)$$

Where a and b were calculated as coefficient parameters. They provided more importance to GU and HPP when computing the HFI. $a = {}^{2}/_{3}$ *and* $b = {}^{6}/_{5}$, respectively.

Based on the observations for x from twenty

participants of this study, and some test results published for 1D anthropometric studies using 1st and 99th percentile head measurements of females and males, respectively from different ethnic groups (Zhuang and Bradtmiller, 2005); (International Organization for Standardization, 2010a), we anticipated that x would rarely exceed the 30 mark and would represent an extremely low fit. We, therefore, decided to assign 0.1 to λ and multiplied the function by 1000 to define the HFI function as shown Figure 13 (e.g. with $x = 30$, $HFI = 5$).

$$HFI: \begin{matrix} [0;\infty) \to (0;100] \\ x \mapsto 100 * \exp(-0.1x) \end{matrix} \quad (3)$$

Replacing x in (3) and rounded up to 2 decimal points gives:

$$HFI = \begin{cases} 100 * \exp\left(0.13 - \frac{|SOD-6|}{15} - \frac{0.12GU}{HPP}\right) \\ \qquad for\ 4 > SOD > 8 \\ 100 * \exp\left(-\frac{0.12GU}{HPP}\right) \\ \qquad for\ 4 \le SOD \le 8 \end{cases} \quad (4)$$

Similarly, a HFI score was developed for local regions based only on the local SOD and GU. The proposed equation was:

$$HFI_{local} = \begin{cases} 100 * \exp\left(0.13 - \frac{|SOD-6|}{15} - 0.12GU\right) \\ \qquad for\ 4 > SOD > 8 \\ 100 * \exp(-0.12GU) \\ \qquad for\ 4 \le SOD \le 8 \end{cases} \quad (5)$$

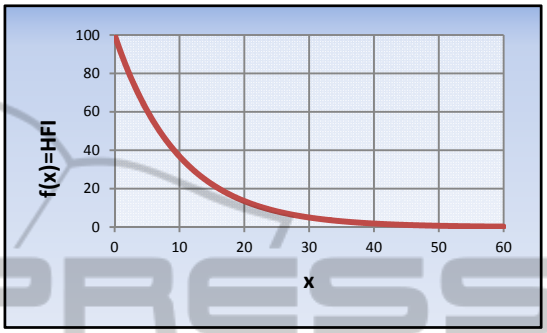

Figure 13: HFI graph.

Table 1: Overall fit parameter values for 20 participants.

No.	Gender	Helmet Size	Hair Thickness (mm)	SOD (mm)	GU (mm)	Test Area (mm^2)	Actual Helmet Protection Area (mm^2)	HPP	x	HFI
1	Male	Medium	3.35	6.76	3.40	66190	56610	0.855	4.8	62.1
2	Male	Large	0.11	15.61	7.60	76670	46530	0.607	20.1	13.4
3	Female	Medium	3.36	11.06	4.34	62150	50680	0.815	8.5	42.9
4	Male	Large	3.22	10.50	4.36	70400	56350	0.800	8.2	43.9
5	Male	Medium	3.79	9.17	4.11	66820	52570	0.787	7.1	49.3
6	Male	Medium	4.46	8.11	2.98	68840	54830	0.796	4.6	63.2
7	Female	Large	9.22	16.94	7.34	63640	55320	0.869	16.1	19.9
8	Male	Large	1.44	9.58	4.68	63240	53980	0.854	7.7	46.5
9	Male	Large	3.74	12.02	4.64	63140	54920	0.870	9.1	40.2
10	Male	Medium	4.36	7.73	3.31	62430	54680	0.876	4.5	63.5
11	Male	Large	2.88	9.28	3.67	72060	56265	0.781	6.5	52.1
12	Female	Medium	4.41	8.97	3.48	63170	54340	0.860	5.5	57.5
13	Male	Large	1.22	9.07	3.70	62740	54590	0.870	5.8	55.7
14	Male	Medium	2.04	7.41	3.33	67190	53700	0.799	5.0	60.7
15	Male	Large	7.62	14.17	5.18	67420	56733	0.841	11.5	31.6
16	Female	Medium	2.98	10.37	5.55	54030	51140	0.947	8.6	42.1
17	Male	Medium	2.88	7.12	3.59	75030	53415	0.712	6.1	54.6
18	Female	Medium	7.35	10.17	3.74	64680	57100	0.883	6.6	51.9
19	Male	Medium	5.96	5.98	2.92	72780	53640	0.737	4.8	62.1
20	Male	Medium	4.10	10.96	5.09	61450	51430	0.837	9.3	39.4
Mean			3.92	10.05	4.35	66204	53941	0.820	8.0	47.6
Standard Deviation			2.23	2.88	1.30	5342	2543	0.074	4.0	14.0

3 RESULTS

Participants were 15 males and 5 females, aged between 21 to 37 years (mean = 26.2 ± 4.5), took part in the pilot study to evaluate the feasibility of the method, and the performance and strength of the HFIs. The participants were asked to try and select the best perceived helmet fit between two sizes of the same model (Met Kaos size Medium and Large) before the start of the experiment. Table 1 presents the results for the computed hair thickness, SOD, GU, HPP, x and HFI for each participant. The parameters means and standard deviations are presented in the last two rows of Table 1.

Fit parameters for the five local regions are presented in table 2 with respective SODs, GUs and HFIs.

4 DISCUSSION

The global HFI distribution from Table 1 shows two extreme poor fit for participant No. 2 and No. 7 (HFI=13.4 and 19.9 respectively) with large SODs and Gus. Only 60.7% of the head test area for participant No. 2 was protected by the helmet. The other 18 HFIs ranged from 31.6 to 63.5 with a mean value of 47.6 (±14.0). It is apparent from Table 1 that the GUs are large, indicating a non-uniform distribution of the gap throughout the head length.

Local gap distribution showed slight dissimilarities between the five regions, with the back region providing the bigger gaps (SOD) and a worst fit (HFI) than the other helmet regions.

Further analysis with larger samples in both number of participants and helmet models is deemed necessary to establish the validity of these observations. The pilot study will help in the determination of the sample size for future helmet fit analyses involving the HFI.

An exponential distribution is believed to have a better impact on the index strength rather than a linear distribution. It gives less amplitude to very poor fit ($\sim x > 15$) and more dissimilarity to small variation when x gets closer to zero. For this reason,

Table 2: Local fit parameter values for 20 participants.

No.	Front			Top			Right			Left			Back		
	SOD (mm)	GU (mm)	HFI	SOD (mm)	GU (mm)	HFI	SOD (mm)	GU (mm)	HFI	SOD (mm)	GU (mm)	HFI	SOD (mm)	GU (mm)	HFI
1	5.04	2.31	75.8	8.27	3.29	66.0	6.23	3.15	68.5	6.03	3.36	66.8	9.20	3.18	62.8
2	6.50	4.29	59.8	23.31	5.84	17.8	17.44	5.42	27.7	15.12	4.69	35.3	9.73	4.30	53.0
3	12.03	4.62	43.8	7.19	4.62	57.4	12.25	2.31	56.9	13.19	2.82	50.3	10.73	3.96	51.7
4	7.98	4.18	60.6	9.67	4.83	49.9	9.94	2.56	64.4	12.84	3.78	45.9	13.55	4.50	40.1
5	13.39	2.67	50.5	6.47	3.63	64.7	8.61	3.51	62.8	8.59	2.75	68.9	11.24	4.69	45.7
6	8.24	2.66	71.3	7.35	4.17	60.6	8.94	2.62	68.4	8.45	1.68	79.1	6.93	2.48	74.3
7	15.81	4.31	35.3	11.95	6.47	35.2	17.23	5.73	27.1	18.75	7.04	20.9	27.14	6.47	12.8
8	9.09	4.19	56.1	7.93	4.16	60.7	8.68	3.61	61.8	10.28	4.32	51.0	16.34	2.81	40.8
9	9.55	3.90	56.3	9.13	5.34	48.7	13.72	2.96	47.7	13.61	3.35	45.9	15.83	3.77	37.6
10	7.99	2.23	76.5	6.86	3.94	62.3	8.00	3.11	68.9	6.91	2.90	70.6	10.78	2.54	61.1
11	8.42	4.49	56.5	8.54	4.61	55.3	9.66	2.60	65.3	10.34	2.88	60.4	9.99	2.63	63.7
12	12.57	2.61	53.7	7.47	4.00	61.9	8.82	2.63	68.8	8.48	2.04	75.6	8.01	3.85	62.8
13	9.41	3.07	62.8	7.31	4.60	57.6	8.78	2.30	71.8	9.91	3.51	57.6	12.18	3.03	52.4
14	7.49	3.50	65.7	7.21	3.70	64.1	8.95	2.00	73.6	6.96	3.08	69.1	5.13	3.61	64.8
15	15.52	2.79	43.2	9.81	4.89	49.1	14.84	4.25	37.9	14.19	3.92	41.2	21.77	3.52	26.1
16	15.46	2.93	42.6	6.66	3.80	63.4	8.84	4.58	54.4	8.69	4.12	58.1	18.48	3.06	34.3
17	10.42	2.65	61.7	8.16	3.75	62.9	5.97	3.34	67.0	4.86	2.52	73.9	7.39	1.82	80.4
18	9.12	2.57	67.9	8.00	4.24	60.1	11.37	2.89	56.3	10.68	2.6	61.0	13.14	2.73	51.0
19	5.66	2.90	70.6	6.03	3.74	63.8	6.11	1.84	80.2	7.05	2.13	77.4	3.60	3.07	67.1
20	16.39	2.86	40.4	8.44	3.37	64.6	9.28	4.02	56.5	8.76	3.42	62.9	17.15	2.09	42.1
ME	10.30	3.29	57.6	8.79	4.35	56.3	10.18	3.27	59.3	10.18	3.35	58.6	12.42	3.41	51.2
SD	3.50	0.80	12.1	3.68	0.82	11.8	3.34	1.07	14.4	3.49	1.17	15.3	5.75	1.06	16.7

we decided to base the HFI on the exponential distribution rather than the x value.

We acknowledged there were some limitations for the presented method. First, we assumed that the participants' hair were fully flattened under the helmet compression and did not affect the fit score. While this might be the case for most cyclists, HFI for people with very thick, bulky and curly hair will produce erroneous results. Also, a uniform hair thickness across the participant's head might not be accurate. People with some baldness may only have hair on the side of the head, while others may have asymmetric haircuts with non-uniform hair distribution.

Despite the limitations, our findings showed that the HFI method did provide accurate and efficient data to analyse, compare and improve bicycle helmet fit amongst the cyclist population considered. Further studies are however required to gather deeper insights on the HFI prospective.

5 CONCLUSIONS

The paper focuses on bicycle helmet fit that closely influences the wearer's safety during crashes involving head impact. A computational analysis method has been developed to help quantifying how closely the contour of a helmet liner follows the head shape of an individual. The HFI was introduced and found to be a plausible accurate tool for fit analysis. Such information was relevant and useful and might be taken into consideration in both helmet development and testing.

This study is part of a larger project emphasising on helmet comfort and safety assessment from random sampling of the Australian cycling community. It aims at improving helmet fit and hence safety through mass-customisation.

REFERENCES

Abu-Zidan, F. M., Nagelkerke, N. & Rao, S. 2007. Factors Affecting Severity Of Bicycle-Related Injuries: The Role Of Helmets In Preventing Head Injuries. *Emerg Med Australas,* 19**,** 366-71.

Attewell, R. G., Glase, K. & Mcfadden, M. 2001. Bicycle Helmet Efficacy A Meta-Analysis. *Accident Analysis And Prevention,* 33**,** 345-352.

Ball, R. 2009. 3-D Design Tools From The Sizechina Project. *Ergonomics In Design: The Quarterly Of Human Factors Applications,* 17**,** 8-13.

British Standards Institution 2006. Bs En960:2006. Headforms For Use In The Testing Of Protective Helmets.

Cripton, P. A., Dressler, D. M., Stuart, C. A., Dennison, C. R. & Richards, D. 2014. Bicycle Helmets Are Highly Effective At Preventing Head Injury During Head Impact: Head-Form Accelerations And Injury Criteria For Helmeted And Unhelmeted Impacts. *Accid Anal Prev,* 70c**,** 1-7.

Hagel, B. E., Lee, R. S., Karkhaneh, M., Voaklander, D. & Rowe, B. H. 2010. Factors Associated With Incorrect Bicycle Helmet Use. *Inj Prev,* 16**,** 178-84.

International Organization For Standardization 2010a. Iso7250-2 Basic Human Body Measurements For Technological Design,.

International Organization For Standardization 2010b. Iso 20685:2010(E) 3-D Scanning Methodologies For Internationally Compatible Anthropometric Databases.

Meunier, P., Tack, D., Ricci, A., Bossi, L. & Harry, A. 2000. Helmet Accommodation Analysis Using 3d Laser Scanning. *Applied Ergonomics,* 31**,** 361-369.

Rivara, F. P., Astley, S. J., Clarren, S. K., Thompson, D. C. & Thompson, R. S. 1999. Fit Of Bicycle Safety Helmets And Risk Of Head Injuries In Children. *Injury Prevention,* 5**,** 4.

Robinette, K. M. & Whitestone, J. J. 1994. The Need For Improved Anthropometric Methods For The Development Of Helmet Systems. *Aviation Space And Environmental Medicine,* 65**,** A95-A99.

Romanow, N. R., Hagel, B. E., Williamson, J. & Rowe, B. H. 2014. Cyclist Head And Facial Injury Risk In Relation To Helmet Fit: A Case-Control Study. *Chronic Diseases And Injuries In Canada,* 34.

Standards Australia 2009. As/Nzs 2512.1:2009 Methods Of Testing Protective Helmets *Part 1: Definitions And Headforms.*

Thompson, D. C., Rivara, F. P. & Thompson, R. 1999. Helmets For Preventing Head And Facial Injuries In Bicyclists. *Cochrane Database Syst. Rev*.

Zhuang, Z., Benson, S. & Viscusi, D. 2010. Digital 3-D Headforms With Facial Features Representative Of The Current Us Workforce. *Ergonomics,* 53**,** 661-71.

Zhuang, Z. & Bradtmiller, B. 2005. Head-And-Face Anthropometric Survey Of U.S. Respirator Users. *J Occup Environ Hyg,* 2**,** 567-76.